ELSEVIER

Atmospheric Research 36 (1995) 277–286

ATMOSPHERIC RESEARCH

Use and calibration of Rosemount ice detectors for meteorological research

K.J. Claffey, K.F. Jones, C.C. Ryerson

Snow and Ice Branch, U.S. Army Cold Regions Research and Engineering Laboratory (CRREL), 72 Lyme Road, Hanover, NH 03755-1290, USA

Received 18 October 1993; accepted 17 February 1994

Abstract

Vibrating probe ice detectors made by Rosemount Inc., are used by many researchers for measuring atmospheric icing rates and cloud liquid water contents. The vibration frequency of the probe decreases as ice accretes on it, until the probe is deiced at a factory-set frequency. Rosemount ice detectors are favored because they are readily available, easy to install and simple to operate. They are designed to be used as warning systems for incipient aircraft and antenna icing, and not as precisely calibrated scientific instruments. Calibration cannot be user adjusted, but it can be measured and must be periodically checked if the ice detector is to be used in scientific studies.

We briefly describe three models of Rosemount ice detectors that CRREL has used. Methods for collecting and processing the data from these ice detectors are described and evaluated. Procedures developed at CRREL for calibrating Rosemount detectors against a rotating multicylinder in natural icing conditions are presented. Results of calibrations of two model 872B12 Rosemount ice detectors with the rotating multicylinder are presented and discussed. Use of the ice detector record to calculate cloud liquid water content is described.

1. Introduction

An instrument commonly used to make atmospheric icing measurements is the vibrating probe ice detector made by Rosemount Inc. Ice accretes on an axially vibrating probe, causing the vibration frequency to decrease. When the frequency reaches a predetermined lower limit, a heater melts the accumulated ice. After a preset time the heater turns itself off, and ice can accrete on the probe again. The heater sends out a signal that is recorded on a strip chart or datalogger. Typically, the number of times that the heater operates is reported in heater (de-icing) cycles per hour. In this paper we describe an improved data collection method for Rosemount ice detectors. We also describe procedures developed for calibrating the ice detectors using a rotating multicylinder in natural icing conditions. Once

SSDI 0169-8095(94)00042-5

Table 1
Rosemount ice detector used by CRREL (Rosemount, 1975, 1987, n.d.). All measurements were taken from Rosemount manuals except as noted

Model no.	Probe (cm)		Frequency (Hz)		Length of heater cycle (s)
	Diameter	Length	Resting	Trip	
872DC	0.635	2.54**	40.000	39.865*	7
871CB1	0.635	2.79	40.000	39.800*	90
872B12	0.625*	2.54	40.000	39.867	90

*Measurements determined in the laboratory, not given in manual.
**The manual gives a length of 2.79 cm; however, measurements of the actual instrument indicate a probe length of 2.54 cm.

calibrated, a Rosemount ice detector can be used to compute cloud liquid water content if wind speed is measured and droplet size information is available.

2. Background

CRREL has experience with the three models of Rosemount Inc. (1975, 1987, n.d.) ice detectors shown in Table 1. Each model has its own characteristics. Probe diameter and length are used to determine liquid water content from the ice detector record. The difference in probe diameter among these three models has only a small effect on the collection efficiency of the probes. Of more importance is the difference in the length of time the heater is on. The ice detector is not collecting ice during the heater cycle, so information on the icing regime during that time is lost. While a shorter heater time may seem advantageous, it is doubtful that the 7-s heater cycle of model 872DC completely melts the accreted ice under the high winds and low temperatures associated with moderate to heavy icing. The other notable difference between models is the decrease in frequency required to turn on the heater. One would expect that ice detectors with a greater difference between the rest frequency and the de-icing frequency would accrete a larger mass of ice before de-icing.

3. Data collection

Until recently we collected icing data from the Rosemount ice detectors as the number of heater cycles per hour. Collecting the data this way has two limitations: (1) information on changes in the rate of icing within each hour is lost and (2) the amount of time consumed during the hour by heater cycles is not accounted for. It is important to take this heating time into account as icing continues to occur even though droplets cannot freeze on the ice detector probe during a heating cycle. Ryerson (1988) presented a formula to compensate for the 90-s heater cycle (which allows a maximum of 40 de-icing cycles per hour) in Rosemount models 872B12 and 871CB1:

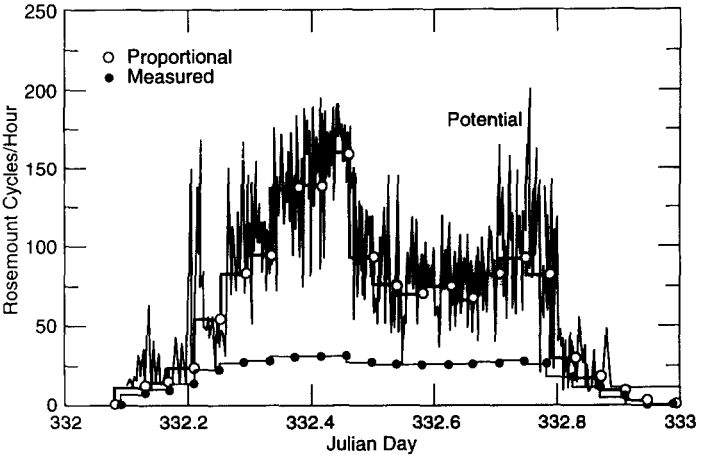

Fig. 1. Time series of measured heater cycles/h (MC), proportional heater cycles/h (PC) and potential icing cycles/h (pc).

$$PC = MC\left\{1 + \frac{MC}{40 - MC}\right\}, \tag{1}$$

where PC is proportional heater cycles per hour and MC is measured heater cycles per hour.

With the availability of better datalogging systems, it is possible to record the time that each heater cycle starts and ends. These recorded times also indicate the icing time for the probe, which is the time between the heater turning off and then turning on again when sufficient ice has accreted. We initially plotted these icing times during icing events, but found that this was not the best way to graphically indicate the severity of icing. Icing time information is best presented if it is inverted. The inverse defines the potential icing cycle rate

$$pc = 1/\text{icingtime}. \tag{2}$$

The inverse of icing time is the potential cycle rate because this is how many icing cycles would occur in a specified time period if the heater cycle were instantaneous. Icing time can be expressed in any units; however, if icing time is expressed in hours the units for pc are cycles per hour, making it directly comparable to PC and MC. In Fig. 1 we compare measured cycles, proportional cycles and potential cycles for one ice detector for one day on Mt. Washington. A close correspondence between proportional and potential cycles can be seen. Note that neither PC or pc takes into account the cooling time of the probe, the time between when the heater turns off and when the temperature of the ice detector probe falls below 0°C and it can again accrete ice. The cooling time will discussed later.

In the following sections the potential cycle rate is used in the Rosemount ice detector probe calibration and in the calculation of cloud liquid water content from ice detector data.

4. Rosemount calibration

Output from the Rosemount ice detector presented in terms of an icing cycle rate is useful for indicating how severe icing conditions are. Ultimately, one would like to use the ice

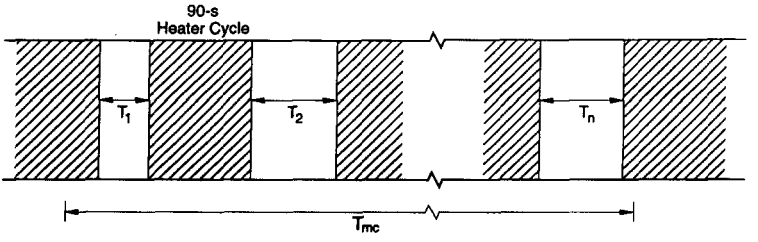

Fig. 2. Rosemount icing cycles T_i during multicylinder run T_{mc}. Heater cycles (shown hatched) are all 90 s long.

detector to measure the variation of cloud liquid water content at a site. This requires that the ice detector be calibrated to determine the mass of ice that accretes on the probe during each icing cycle. We have developed a calibration method for the Rosemount using the rotating multicylinder in natural icing conditions. We have calibrated Rosemount ice detectors at the Mt. Washington Observatory for three one-week periods in the past two years. The results presented here are for two Rosemount model 872B12's calibrated during the week of November 26 to December 1, 1992. During this calibration week there were 4 days during which icing occurred. Air temperature and wind speeds during calibrations ranged from -5°C to -11°C and from 7 to 32 m s^{-1}, respectively.

The rotating multicylinder method for determining cloud liquid water content (LWC) and median volume droplet diameter (MVD) by measuring the mass of accreted ice on six cylinders of different diameters is explained in Howe (1991). In our multicylinder runs we follow Howe's procedure except that we determine LWC and MVD using a computer program based on Finstad and Lozowski (1988) adapted to the Mt. Washington Observatory. Of the 6 cylinders on the multicylinder, 0.5-cm-diameter cylinder 2 is the closest in diameter to the 0.625-cm-diameter Rosemount probe. While cylinder 2 is smaller than the Rosemount probe, typical ice accretion diameters on that cylinder at the end of a multicylinder run are between 0.75 and 0.9 cm. The increase in iced diameter of cylinder 2 during a multicylinder run causes a decrease in its collection efficiency. For example, at a wind speed of 14.8 m s^{-1} and an MVD of 13.5 mm, the collection efficiency of cylinder 2 decreases from 0.59 when the cylinder is bare, to 0.50 at an iced diameter of 0.7 cm, and to 0.43 at an iced diameter of 0.9 cm. For the same wind speed and MVD the collection efficiency of the bare Rosemount probe is 0.54. As the probe does not rotate and accretes only a small amount of ice before de-icing, its collection efficiency remains essentially constant during an icing cycle. In using the multicylinder to calibrate Rosemount ice detectors, we are assuming that the ice accretion rate on cylinder 2 and the Rosemont probe are the same. For the typical conditions above, the cylinder 2 ice accretion rate ranges from 87% of the Rosemount probe ice accretion rate when it is bare, to 104% at a 0.7-cm iced diameter, to 114% at a 0.9-cm iced diameter. This close agreement indicates that the multicylinder can be used to determine the mass calibration for Rosemount probes.

Multicylinder exposure times are typically between 5 and 20 minutes and include between 3 and 6 ice detector cycles. A multicylinder run, with concurrent Rosemount icing and heater cycles, is shown schematically in Fig. 2.

For each multicylinder run, we calculated the average potential cycle rate for each individual ice detector:

Table 2
Ice detector calibration data for 44 multicylinder runs. The bold italicezed values were not used to compute means. See text for explanation

Run	Start time (Jul. day)	T_{mc} (min)	m_2 (g)	L_2 (cm)	sn 205		sn226	
					$\overline{pc}$ (l/min)	m_r (g)	$\overline{pc}$ (l/min)	m_r (g)
1	332.19	8.18	6.08	9.20	0.344	***0.597***	2.258	***0.091***
2	332.26	7.63	1.47	9.95	1.749	0.028	1.899	0.026
3	332.37	8.82	5.46	10.10	2.490	0.063	2.732	0.057
4	332.42	6.63	4.19	10.05	2.605	0.061	3.330	0.048
5	332.46	6.92	5.18	10.05	2.603	0.073	2.858	0.066
6	332.50	6.77	2.86	10.00	1.008	0.107	1.975	0.054
7	332.58	7.00	2.78	10.10	1.333	0.075	2.005	0.050
8	332.63	8.00	3.20	10.10	1.337	***0.075***	0.980	***0.103***
9	332.67	8.25	3.65	10.05	1.526	***0.073***	0.491	***0.228***
10	332.73	7.27	3.60	10.05	1.334	***0.094***	0.152	***0.826***
11	332.76	6.25	3.46	10.10	1.565	***0.089***	0.114	***1.226***
12	332.85	10.00	2.21	10.05	0.320	***0.174***	0.212	***0.264***
13	334.37	16.52	0.73	10.10	0.230	0.048	0.169	0.066
14	334.43	15.02	2.02	10.10	0.655	0.052	0.744	0.045
15	334.47	15.50	1.61	10.05	0.511	0.051	0.640	0.041
16	334.57	17.05	1.09	10.10	0.307	0.052	0.325	0.049
17	334.59	18.27	1.38	10.10	0.345	0.055	0.394	0.048
18	334.63	18.75	1.24	10.10	0.341	0.049	0.339	0.049
19	334.68	16.73	1.53	10.10	0.555	0.041	0.601	0.038
20	334.71	15.03	1.49	10.10	0.478	0.052	0.520	0.048
21	334.75	15.00	1.43	10.05	0.474	0.051	0.471	0.051
22	334.84	15.03	1.76	10.05	0.597	0.050	0.606	0.049
23	334.89	14.45	1.90	10.05	0.704	0.047	0.759	0.044
24	334.92	14.27	2.50	10.10	0.806	0.055	1.090	0.040
25	334.98	12.50	1.90	10.05	0.850	0.045	0.045	0.037
26	335.02	11.87	2.34	10.05	1.046	0.048	1.926	0.026
27	335.06	11.50	2.56	10.10	1.121	0.050	1.581	0.035
28	335.10	9.87	2.73	10.05	1.319	0.053	2.041	0.034
29	335.13	8.50	2.22	10.05	1.294	0.051	2.278	0.029
30	335.18	8.17	2.19	10.05	1.109	0.061	1.390	0.049
31	335.72	8.68	1.11	10.05	0.585	0.055	0.562	0.057
32	335.76	15.87	1.33	10.10	0.430	0.049	0.460	0.046
33	335.84	18.33	5.77	10.15	1.453	0.054	2.207	0.036
34	335.91	8.08	2.83	10.10	1.583	0.056	2.565	0.034
35	335.96	7.00	2.92	10.10	1.966	0.053	3.090	0.034
36	336.01	7.02	3.14	10.15	2.237	0.050	2.815	0.040
37	336.06	5.92	1.29	10.05	1.212	0.045	2.377	0.023
38	336.10	7.08	3.20	10.05	1.797	0.064	2.623	0.044
39	336.14	6.92	3.09	10.05	1.274	***0.089***	2.267	0.050
40	336.18	6.17	3.31	10.10	1.244	***0.109***	2.961	0.046
41	336.24	5.25	2.62	10.05	1.804	0.070	2.984	0.042
42	336.28	5.00	1.97	10.10	2.000	0.050	2.376	0.042
43	336.32	5.25	1.83	10.10	1.443	0.061	2.201	0.040
44	336.40	21.75	0.87	10.10	0.184	***0.055***	0.047	***0.214***
					Mean ice mass/cycle	0.055		0.044
					Standard deviation	0.012		0.010

$$\overline{pc} = \frac{1}{n}\left\{\frac{1}{T_1} + \frac{1}{T_2} + \frac{1}{T_3} + \ldots + \frac{1}{T_n}\right\} \tag{3}$$

where n is the total number of Rosemount icing cycles during the multicylinder run and T_i is the duration of each Rosemount icing cycle. In cases where the multicylinder run started or ended during an icing cycle, the icing cycle was included in the average if more than half of it occurred during the multicylinder run. The mass per potential cycle of the Rosemount for the jth multicylinder run m_{rj} is calculated by multiplying the mass of ice accreted on cylinder 2 of the multicylinder by the ratio of the length of the Rosemount probe to the length of cylinder 2, and by the ratio of accretion times on the Rosemount probe and the multicylinder, resulting in:

$$m_{rj} = m_2 \frac{L_r}{L_2} \frac{1/\overline{pc_j}}{T_{mcj}}, \tag{4}$$

where m_2 is the mass of ice on cylinder 2, L_2 = length of the ice accretion on cylinder 2, L_r = the length of the Rosemount probe, T_{mcj} = duration of the jth multicylinder run, $\overline{pc_j}$ = average potential cycle rate for the jth multicylinder run.

For each ice detector the average mass per potential cycle $\overline{m_r}$ for the multicylinder runs for the calibration period was determined. The calibration data for Rosemounts sn205 and sn226 are shown in Table 2. Three of the 44 multicylinder runs during this week, runs 1, 9 and 44, were omitted from the calculated $\overline{m_r}$ because of the low quality of those runs. Runs 8 through 12 were omitted because of questionable Rosemount data (ice may have built up around the probes), and for Rosemount sn205, runs 39 and 40 were omitted because during those runs that ice detector behaved differently from the other four that were being calibrated. For Rosemounts sn205 and sn226, $\overline{m_r}$, values are 0.055 and 0.044 g cycle^{-1} respectively. The standard deviation of $\overline{m_r}$ for both probes is about 0.01 g cycle^{-1}.

5. Liquid water content

Using this mass calibration for the Rosemounts, along with wind speed and droplet size data, cloud liquid water content W can be determined from

$$W = \frac{m}{EVD_r L_r T}, \tag{5}$$

where m = mass of ice accreted on the probe, E = collection efficiency of the probe, V = wind speed, D_r probe diameter, L_r = probe length, T = duration of icing period. Substituting $\overline{m_r}$ for mass and pc for $1/T$ in Eq. (5) results in:

$$W = \frac{\overline{m_r} pc}{EVD_r L_r} \tag{6}$$

The effect on calculated LWC of ignoring the cooling time of the probe can be seen by examining this equation. If the cooling time were subtracted from our icing time (to give the true icing time) the average potential cycle rate for each multicylinder run would be

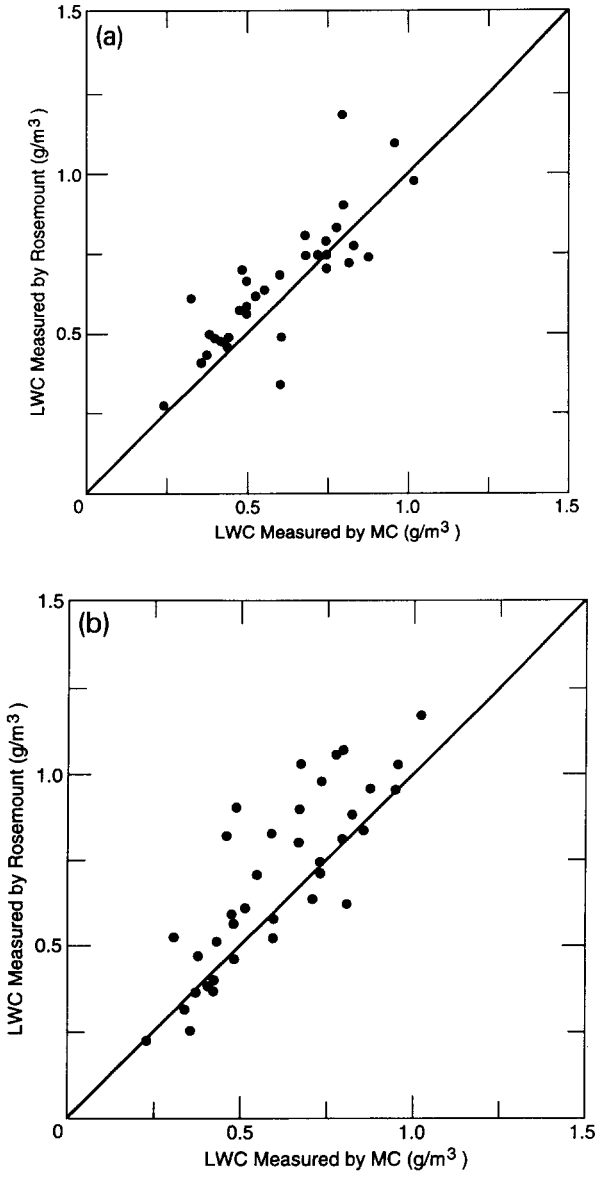

Fig. 3. a. Liquid water content as computed by multicylinder (*MC*) and ice detector sn205 during multicylinder runs using measured *MVD*. b. Liquid water content as computed by multicylinder (*MC*) and ice detector sn226 during multicylinder runs using measured *MVD*.

larger, resulting in a smaller m_r (Eq. 4). However, this is compensated for by the larger *pc* that would be used in determining liquid water content in Eq. 6. It can be shown that if the cooling time is proportional to the icing time, then there is no effect on the calculated LWC from ignoring the cooling time. Alternatively if cooling time is small compared to the icing time, then errors due to ignoring cooling time in the calculation of m_r and in *pc* essentially

balance in Eq. (6). This would give a random error in the calculation of liquid water content and may explain some of the scatter in Fig. 3a and b.

6. Verification

Eq. (6) was used to compare LWC computed from the two Rosemount ice detectors with LWC determined by the multicylinder. In the calculation of the Rosemount LWC we used multicylinder-determined droplet diameters to calculate the probe's collection efficiency. Rosemount and multicylinder liquid water contents are compared in Fig. 3a and b for Rosemounts sn205 and sn226 respectively. Ordinarily, droplet diameter would not be known and the collection efficiency of the probe would have to be determined using an estimated or assumed MVD. The measured droplet diameter was used here to show how well the Rosemount detector liquid water content compares to the multicylinder given complete information. It should be noted that while the multicylinder LWC does depend on the mass of ice on cylinder 2, it is primarily determined from the accreted mass on the smallest cylinder. The main contribution of the five larger cylinders of the multicylinder is

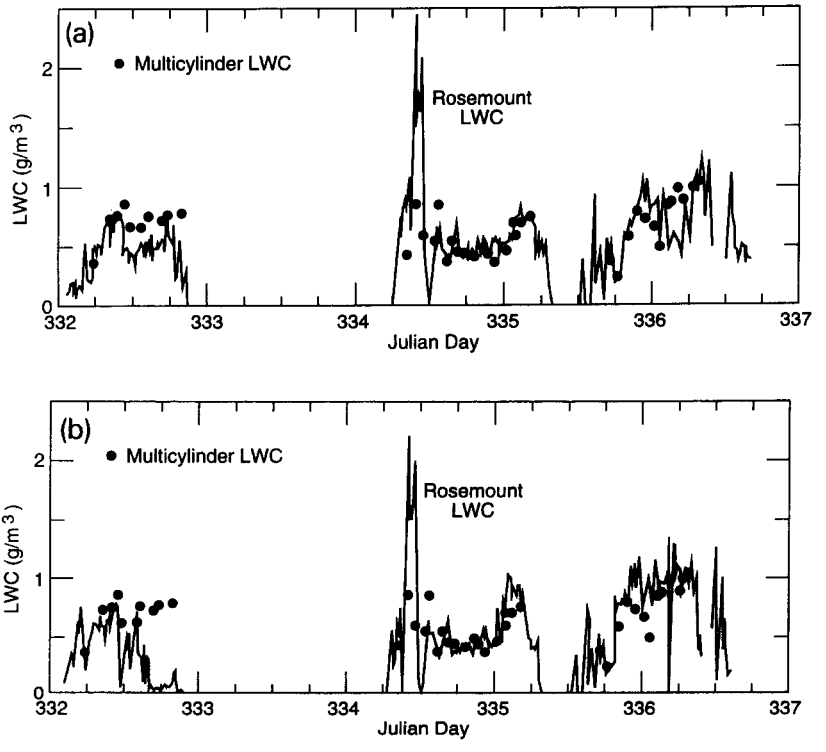

Fig. 4. a. Liquid water content time series of multicylinder and ice detector sn205 assuming an *MVD* of 13.5 mm. b. Liquid water content time series of multicylinder and ice detector sn226 assuming an *MVD* of 13.5 mm.

in determining the MVD. Thus the good agreement between the Rosemounts and the multicylinder liquid water contents shown in these figures goes beyond the quality of the calibration.

A more typical comparison can be made by using an average MVD in the calculation of collection efficiency. In Fig. 4a and b we compare the continuous liquid water content record from Rosemounts sn205 and 226 to the 41 multicylinder measurements made during the same week. The Rosemount potential cycle rates are averaged over 15-minute periods to correspond to the available wind speed information. Because digital wind speed data were not available, average wind speeds were determined by eye from a strip chart record, with low accuracy for wind speeds under about 10 m s^{-1}. Liquid water content measured by the multicylinder and the Rosemounts agree well with a few exceptions. For example, ice detector sn226 disagrees with both the multicylinder and ice detector sn205 during the second half of Julian day 332. This discrepancy may be due to the accretion of ice on the rail around the detector. After this was observed, ice was frequently removed from around the detectors during the remainder of the experiment. The strong disagreement between the multicylinder and both ice detectors during Julian day 334 is probably due to errors in determining the wind speed from the strip chart in the low winds on that day. We expect this disagreement to be resolved when we obtain digital wind speed data from the Mt. Washington Observatory for this week. This points out how critical accurate wind speed data are in determining liquid water content using the Rosemount ice detector.

7. Conclusions and future work

This preliminary analysis of our calibration data indicates that the Rosemount ice detector may be effective for measuring liquid water content at remote sites. However, as seen from the two calibrations presented in this paper, each ice detector is unique and must be individually calibrated before being used. We found that it is important to keep the structure immediately around the detector ice-free so that wind flow around the probe is not impeded. This may require that automatic de-icing equipment be provided at remote sites. The liquid water content time series also emphasized the importance of accurate wind speed data.

There are several questions about the performance of Rosemount ice detectors we plan to investigate further.

There may be a relationship between the frequency decrease required to turn on the probe heater and the mass accreted per icing cycle. This is important not only because Rosemount makes ice detectors with different trip frequencies, but also because it has been our experience that as an ice detector ages its rest frequency decreases. It would be helpful if there were a way to monitor the frequency of the probe as ice accretes. This would provide an indication of drifts in the rest frequency or trip frequency and would also give a better time series resolution of LWC fluctuations.

We would like to get a quantitative measure of the effect of the cooling time of the probe on its calibration. Baumgardner and Rodi (1989) report cooling times between 13 and 24 s for their model 871FA Rosemount probe. This model has a higher power heater and shorter heating time than the Rosemount detectors we use. We would like to measure the cooling

time in natural icing conditions to determine the effects of variations in wind speed, air temperature and LWC.

The Rosemount ice detector, when properly calibrated, appears to be a promising tool for obtaining automated time series of cloud supercooled LWC when accurate wind speed measurements are available. We expect that as the rest of our calibration data are analyzed and additional calibration trials are performed we will have a better understanding of Rosemount ice detectors.

Acknowledgements

The authors wish to thank the staff of the Mt. Washington Observatory. This work was supported by CRREL under Work Units "Icing and Ice Adhesion Fundamentals" and "Mechanical Design for Icing Environments."

References

Baumgardner, D. and Rodi, A., 1989. Laboratory and wind tunnel evaluations of the Rosemount icing detector. J. Atmos. Ocean. Tech., 6: 971–979.

Finstad, K. and Lozowski, E., 1988. Computational investigation of water droplet trajectories. J. Atmos. Ocean. Tech., 5, pp 160–170.

Howe, J., 1991. Rotating Multicylinder Method for the Measurement of Cloud Liquid-Water Content and Droplet Size. CRREL Rep., 91-2, Hanover, NH, 21 pp.

Rosemount Inc., 1975. Instruction Manual 57522C, Ice detector Model 872DC. Minneapolis, MN.

Rosemount Inc., 1987. Instruction Manual D8520101A, Ice detector Model 872B. Minneapolis, MN.

Rosemount Inc., n.d. Instruction Manual 86819, Revision B, Ice detector Model 871CB1. Minneapolis, MN.

Ryerson, C., 1988. Atmospheric icing climatologies of two New England mountains. J. Appl. Meteorol., 27: 1261–1281.